Published in final edited form as:
Biochemistry. 2010 August 3; 49(30): 6317–6328. doi:10.1021/bi100338e.

Characterization of membrane protein non-native states. 1. Extent of unfolding and aggregation of rhodopsin in the presence of chemical denaturants†

Arpana Dutta[1], **Kalyan C Tirupula**[1], **Ulrike Alexiev**[2], and **Judith Klein-Seetharaman**[1,*]

[1]Department of Structural Biology, University of Pittsburgh School of Medicine, Pittsburgh, PA 15260, USA

[2]Freie Universität Berlin, Inst. für. Experimentalphysik, Arnimallee 14, D-14195 Berlin, Germany

Abstract

Little is known about the general folding mechanisms of helical membrane proteins. Unfolded, i.e. non-native states, in particular, have not yet been characterized in detail. Here, we establish conditions under which denatured states of the mammalian membrane protein rhodopsin, a prototypic G protein coupled receptor with primary function in vision, can be studied. We investigated the effects of the chemical denaturants sodium dodecyl sulfate (SDS), urea, guanidine hydrochloride (GuHCl) and trifluoroacetic acid (TFA) on rhodopsin's secondary structure and propensity for aggregation. Ellipticity at 222nm decreases in the presence of maximum concentrations of denaturants in the order TFA > GuHCl > urea > SDS + urea > SDS. Interpretation of these changes in ellipticity in terms of helix loss is challenged because the addition of some denaturants leads to aggregation. Through a combination of SDS-PAGE, dependence of ellipticity on protein concentration and 1D ^{1}H NMR we show that aggregates form in the presence of GuHCl, TFA and urea but not in any concentration of SDS, added over a range of 0.05% to 30%. Mixed denaturant conditions consisting of 3% SDS and 8M urea, added in this order, also did not result in aggregation. We conclude that SDS is able to prevent the exposure of large hydrophobic regions present in membrane proteins which otherwise leads to aggregation. Thus, 30% SDS and 3% SDS + 8M urea are the denaturing conditions of choice to study maximally unfolded rhodopsin without aggregation.

Membrane proteins are essential for all living systems and include important protein families such as receptors, transporters, ion channels, pumps, and proteins with structural roles or enzymatic activity. In humans, membrane proteins constitute one third of all the proteins (1). Failure of a membrane protein to fold into its native three-dimensional structure can lead to disruption of regulated cell functions and cause diseases (2). There are several pathological conditions such as cystic fibrosis, Charcot-Marie-Tooth disease, hearing loss, and Retinitis Pigmentosa (RP), in which misfolding of membrane proteins has been implicated as contributing to disease (2). Through an understanding of the folding mechanism of membrane proteins it may be possible to identify avenues for the treatment of such diseases.

†This work was in part supported by the National Science Foundation CAREER grant CC044917, National Institutes of Health Grant NLM108730, and the Pennsylvania Department of Health.

* To whom correspondence should be addressed: Judith Klein-Seetharaman, Associate Professor, Department of Structural Biology, University of Pittsburgh School of Medicine, Rm. 2051, Biomedical Science Tower 3, 3501 Fifth Avenue, Pittsburgh, PA15260, Tel: 412 383 7325, Fax: 412 648 8998, jks33@pitt.edu.

In the field of soluble proteins, characterization of unfolded states has been crucial in understanding mechanisms of folding and indeed has shed light also on misfolding diseases (3,4). An important conclusion is that even under strongly denaturing conditions some inter-residue interactions, either native-like or non-native and especially those among hydrophobic residues, are present in the unfolded state (5). Such interactions constitute residual structure in denatured states and are assumed to form during the early stages of folding of a protein, playing crucial role for folding by acting as a folding nucleus (5). Non-native interactions of unstructured peptide fragments for example are believed to play a major role in amyloid formation in Alzheimer's disease (6). In principle, any protein sequence has an intrinsic propensity to aggregate, and even form amyloid fibrils (4), but point mutations can enhance this propensity as has been shown for example for transthyretin and lysozyme (7,8). While these mutations do not alter the structure of the folded state, they change structure and stability of unfolded states and result in accumulation of folding intermediates (7,9). Based on the characterization of these folding intermediates, therapeutic strategies have been proposed such as blocking fibrillar growth by β-sheet breaker peptides (10) and stabilizing native structure of these proteins by small molecules (11-13).

In contrast to soluble proteins, little is known about unfolded states of membrane proteins and there have been few efforts to date towards understanding the molecular mechanisms of membrane protein folding in general. It has been proposed in the two-stage hypothesis that the initial stages of folding of helical membrane proteins involve primarily formation of the helices (14,15), while the long-range interactions hypothesis emphasizes contact formation involving residues in loops connecting the helices (16,17). Experimental testing of such mechanistic hypotheses is challenging mainly due to the difficulties in perturbing these protein systems, in which high stability arises from the hydrophobic environment of the membrane. In order to accommodate the hydrophobic nature of membrane proteins, they need to be reconstituted in a detergent or lipid environment to maintain their functionality, which also renders them resistant towards denaturation. In vitro folding/unfolding studies of membrane proteins require optimization of denaturing conditions that would lead to a significant degree of unfolding. Another challenge faced by denaturation experiments is formation of aggregates due to exposure of large hydrophobic regions of membrane proteins.

The first work on the folding of membrane proteins was carried out with bacteriorhodopsin (bR) which was successfully refolded into phospholipids via transfer into sodium dodecyl sulfate (SDS) micelles after denaturation by trifluoroacetic acid (TFA) (18). This has established bR as a model system for studying the folding of helical membrane proteins (19). Kinetic studies of refolding of bR from an SDS-denatured state into lipid/detergent micelles have enabled detection of folding intermediates in its folding pathway (20-24). Efforts on elucidating the folding pathways of other membrane proteins are underway. Refolding has been possible for the bacterial membrane proteins KcsA, from a trifluoroethanol (TFE)-denatured state (25); DAGK and DsbB from SDS-denatured states (26,27) and EmrE from a SDS+urea denatured state (28) and for the LHCII complex from higher plants from a SDS denatured state (29,30). In all of these cases, however, refolding was accomplished only from a partially unfolded, near native state. Recently, studies with opsin in phospholipid bicelles revealed a significant decrease of 50% in its helical content in the presence of urea, but it could not be refolded from such a largely unfolded state (31). Therefore, refolding of membrane proteins except bR is typically feasible only from a minimally denatured state which is structurally very similar to the native state but becomes difficult when large portions of the structure are unfolded.

While reversibility of unfolding is crucial for kinetic and thermodynamic studies of folding, it is not a requirement for biophysical characterization of denatured states. Here, the

requirements are long-term stability of the denatured state of interest without aggregation. Further, the extent of unfolding is important. To catch a glimpse of the earliest stages in folding, ideally the protein is denatured to the maximum possible extent. In this paper, we therefore describe our efforts on chemical denaturation of rhodopsin in dodecyl maltoside (DM) detergent micelles by addition of SDS, TFA, urea and GuHCl. We find that 4M TFA disrupts secondary structure of rhodopsin to the greatest extent, followed by 8M GuHCl, 10M urea, 3% SDS+8M urea and 30% SDS in decreasing order in their extent of denaturation. However, aggregation of rhodopsin in the presence of urea, GuHCl and TFA precludes further investigation of these denatured states. In contrast, 30% SDS and 3% SDS +8M urea are found to be the most suitable denaturants to study unfolding of rhodopsin due to their largest extent of denaturation without formation of aggregates. As per our knowledge, this is the first time that unfolding and detection of aggregates of a membrane protein has been described in a systematic manner.

Materials and methods

Materials

SDS (electrophoresis grade) was purchased from Biorad (Hercules, CA), dodecyl maltoside (DM) from Anatrace (Maumee, OH). Rhodopsin was isolated from bovine retinae and purified in 2mM sodium phosphate buffer, pH 6 in the presence of 0.05% DM as described previously (32).

Methods

Circular dichroism spectroscopy

CD spectra were recorded using a Jasco J-810 spectrometer (Jasco Inc., Easton, MD). 1.5μM rhodopsin in 2mM sodium phosphate buffer, pH 6 and 0.05% DM in the presence of different concentrations of denaturants was placed in a 1mm quartz cell. All spectra were recorded at 25°C with a bandwidth of 1nm, scan speed of 100nm/min and a response time of 1 second. Each spectrum was reported as an average of ten spectra. Spectra recorded in the absence of denaturant and in the presence of up to 3% SDS, 3M urea and 3M GuHCl were subtracted from the corresponding buffer reference spectra containing 70μM nonamer peptide used during rhodopsin purification. For spectra of solutions containing more than 3% SDS, 3M urea, 3M GuHCl and all concentrations of TFA, sodium phosphate buffer containing 0.05% DM and appropriate denaturant concentration without nonamer were subtracted. This was because very small volumes of highly concentrated rhodopsin were added to the working solution to achieve a final concentration of 1.5μM resulting in dilution of the nonamer to levels undetectable by CD spectroscopy. Note that while the subtraction of nonamer peptide affects ellipticity at 208nm, the change in ellipticity at 222nm is small and amounts to a maximum decrease in absolute ellipticity of about 5% (for 70μM peptide, Figure 1). Most solutions contained less concentrations of the peptide. The effect of denaturants over time was monitored by recording CD scans every 0.5 hours for a period of 14 hours. All CD spectra were analyzed using CDPro software (33). The helicity was estimated by using CDPro by taking the basis set (# 10) containing both soluble proteins and membrane proteins (33).

A python script was developed in the lab as user interface for running CDPro. The script takes as input the CD spectra in millidegrees (θ), path length of cuvette (l in cm), concentration of protein (c in Molar units) and number of amino acids in protein (n) and calculates molar circular dichroism or delta epsilon ($\Delta\varepsilon = \theta/(10*l*c*n*3298)$) which is used as input to CDPro software. The script by default executes all the three secondary structure determining algorithms CONTIN/LL (33,34), SELCON3 (35) and CDSSTR (36) available

with CDPro. There is also an option provided in the script for the user to choose either the basis set suggested by CDPro or to use all available basis sets for data processing. The script generates two plain text (comma separated value format) files: (1) wave length versus calculated mean residue ellipticity ($[\theta] = \Delta\varepsilon*3298$) and (2) re-formatted output of CDPro that can be opened by any spread sheet or plotting programs for further analysis. This script is available at http://jks-lab.structbio.pitt.edu/CD.

SDS-Polyacrylamide gel electrophoresis (SDS-PAGE)

SDS-PAGE analysis of rhodopsin at different denaturant concentrations was performed at 200V for 30min on a 10% SDS-PAGE. SDS concentration was 0.1% in the buffers used to make the stacking and resolving parts of the gel. The electrophoresis buffer also contained 0.1% SDS. Non-reducing Laemmli dye (Biorad, Hercules, CA), consisting of 62.5mM Tris, pH 6.8, 2% SDS, 25% Glycerol and 0.01% Bromophenol Blue was used in 1:1 ratio to load native rhodopsin on the gel. The effect of additional SDS in the non-reducing Laemmli dye on denatured samples was negated by the use of native gel loading dye. The latter in 2X concentration contained 25% glycerol and 0.01% bromophenol blue and was used to load denaturant (SDS and/or urea) containing samples of rhodopsin on the gel. Silver staining was done using SilverSNAP Stain kit (Thermo Scientific, Waltham, MA).

One-dimensional ^{1}H NMR

All NMR measurements were performed at 25°C using a Bruker 800MHz spectrometer. Samples containing 50μM of rhodopsin in 20mM sodium phosphate buffer (pH 6.0), 1% DM and 10% D_2O in presence and absence of SDS were used to record the NMR spectra. One-dimensional ^{1}H NMR spectra were recorded using a selective excitation scheme with sculpting that utilizes a double pulse field gradient spin echo sequence (DPFGSE) as described previously (37,38). A total of 2048 scans were averaged to obtain the final spectrum at each condition. A line broadening of 1Hz was used to process final spectra.

Cysteine accessibility measurements

4,4'-dithiodipyridine (4-PDS) reacts with free sulfhydryl groups in cysteines to produce stoichiometric amounts of 4-thiopyridone that absorbs at 323nm (39) and the reaction was used to quantify cysteine accessibility of rhodopsin essentially as described (40). The number of cysteines reacting with 4-PDS per molecule of rhodopsin was estimated by taking the ratio of the absorbance at 323nm and that at 500nm and multiplying it with the ratio of the molar extinction co-efficient of rhodopsin ($40{,}600 M^{-1}cm^{-1}$) and that of 4-thiopyridone ($19{,}000 M^{-1}cm^{-1}$). 1.5μM rhodopsin in 2mM sodium phosphate buffer, pH 6 and 0.05% DM was reacted with 37.5μM 4-PDS in the sample cuvette at 25°C. The same amount of 4-PDS was added to the reference cuvette. The reaction was followed spectrophotometrically by recording the changes in absorbance spectra over time. At the end of the experiment, when the 323nm peak reached saturation, all spectra were subtracted from the original rhodopsin spectrum in the absence of 4-PDS.

Steady-state Fluorescence Spectroscopy

Fluorescence measurements were carried out using a Varian Cary Eclipse fluorescence spectrophotometer (Varian Inc., Palo Alto, CA). Emission scans of 1.5μM rhodopsin in 2mM sodium phosphate buffer, pH 6 and 0.05% DM titrated with GuHCl were recorded in the wavelength range 310nm-500nm with an excitation wavelength of 295nm. Excitation and emission slit widths were kept at 5nm and 10nm, respectively. Medium photomultiplier tube voltage was applied and measurements were taken at a scan rate of 600nm/min. For time course measurements, fluorescence emission at 330nm was recorded every 30min. All experiments were carried out at 25°C.

Results

Secondary structure of rhodopsin in the presence of different chemical denaturants (SDS, urea, GuHCl, TFA, and combinations thereof) was assessed by circular dichroism. While solvent background precluded measurements at very low wavelengths for some of the conditions, at the very minimum the range including ellipticity at 222nm - most important for assessment of helical structure content - was obtained for all conditions. For each denaturant, we also established whether or not aggregation occurs. Here, the methods varied depending on the denaturant because some approaches are not applicable to some denaturants. The results are summarized in Table 1 and are described below in order of denaturant. Thus, for each denaturant, there is a description of the effects on secondary structure, followed by the effects on rhodopsin aggregation.

SDS as a denaturant of rhodopsin: disruption of secondary structure

To measure the loss of secondary structure in the presence of increasing amounts of SDS, rhodopsin was titrated with varying concentrations of SDS and the circular dichroism (CD) spectrum was recorded at each concentration. CD spectra of rhodopsin (1.5μM) alone and in the presence of low concentrations of SDS up to 3% are shown in Figure 1.A. and those in the presence of high SDS concentrations up to 30% are shown in Figure 1.B. The corresponding plots of mean residue ellipticity (MRE) at 222nm are shown in Figure 1.C. and 1.D., respectively. The magnitude of MRE at 222nm decreases abruptly at a concentration of 0.05% SDS and then remains essentially constant with increasing SDS concentrations until 3% (Figure 1.C.). The decrease in the magnitude of MRE at 222nm at 3% SDS is 12±2% which corresponds to an estimated ~19% decrease in helicity calculated using CDPro software (33). However, already at 2% SDS, a slight increase in the magnitude of MRE begins which reaches a maximum at 10% SDS (Figure 1.D.). Subsequently, a large decrease in the magnitude of MRE values at 222nm is observed as the SDS concentration is raised beyond 10% up to 30% as shown in Figure 1.D. The change in MRE at 222nm is 39±6% at 30% SDS indicating loss of substantial amounts of native helical regions. The corresponding decrease in helicity, as approximated using CDPro software, is ~45%.

In order to ensure that the values recorded at each SDS concentration correspond to the maximal denaturation by SDS at that concentration, rhodopsin was incubated with 0.05%, 1.5%, 3% and 30% SDS overnight at 25°C. Loss of secondary structure was monitored by CD spectroscopy every 30min during the incubation period but no time dependent further denaturation was observed (data not shown).

The changes in CD spectra (shown in Figure 1.A.) with increasingly higher concentrations of SDS added to rhodopsin are summarized in Figure 1.C. by mean ellipticity at 222nm as a function of SDS concentration. SDS concentrations up to 3% show two distinct stages, an initial decrease in helicity followed by no change up to 3% SDS. The CD results at higher SDS concentrations are shown in Figure 1.B. and 1.D. A third stage over the range of SDS concentrations 3% to 10% SDS can be clearly seen in the CD spectrum in Figure 1.B. and summarized in Figure 1.D.: a distinct increase in the magnitude of MRE at 222nm is observed in this range. In a fourth stage (15% to 30% SDS), a sudden decrease in helicity to a large extent at concentrations beyond 15% SDS.

SDS as a denaturant of rhodopsin: Detection of aggregates

The above studies strongly suggest that high concentrations of SDS are very well suited to denature rhodopsin. In order to be able to characterize the molecular nature of such states, it is imperative that no aggregation occurs in the presence of SDS. We therefore tested for

aggregation using multiple complementary methods, including SDS-PAGE, dependence of molar ellipticity on rhodopsin concentration, and ^{1}H NMR spectroscopy.

First, we looked for aggregates on SDS-PAGE (Figure 2.A. and 2.B.). Native loading dye (see Methods) was used so that no additional amount of SDS is introduced from the sample loading buffer and the result is not an effect of its addition. This is especially critical for the samples containing low concentrations of SDS such as 0.05%, 1% and 3%. The possibility that SDS present in the gel and running buffer (0.1% SDS in each) would dissolve the aggregates we are trying to detect is highly unlikely. This is because we are detecting for aggregates caused by SDS denaturation, i.e. the samples already contain SDS and if aggregates are present they would be dissolved in the sample even before loading on the gel. Further, the amount of SDS that we have used to denature rhodopsin is significantly higher than what is present in the gel and running buffer thus ruling out the contribution of SDS in the gel system, other than that in the samples, to influence our results.

Figure 2.A. shows a silver stained polyacrylamide gel with native rhodopsin in lane 2 (Rho). Native rhodopsin runs as a band between 37kDa and 25kDa on SDS-PAGE and the same gel shows rhodopsin denatured with 0.05%, 1% and 3% SDS in lanes 3, 4 and 5, respectively. These samples were loaded using native loading dye (see Methods). As can be seen from these gels, a single band at the same position as native rhodopsin is observed for rhodopsin in the presence of different concentrations of SDS tested indicating no changes in electrophoretic mobility of SDS-denatured states compared to that of native rhodopsin. The adjacent gel shows rhodopsin denatured with 10%, 20% and 30% SDS in lanes 2, 3 and 4 respectively as compared to native rhodopsin (Rho) in lane 8. These samples were also loaded with native dye (see Methods). To check the stability over time, rhodopsin was incubated with 30% SDS for 2h (lane 5), 12h (lane 6) and 24h (lane 7). A single band in the same position as that of native rhodopsin was also observed during longer incubation of rhodopsin in the presence of 30% SDS, suggesting that SDS-denatured rhodopsin is stable over long periods of time and no aggregation is observed even after 24h of incubation. Rhodopsin denatured by heating at 70°C in lane 9 was run as a positive control for aggregation. In contrast to the lack of aggregation in the presence of SDS, the positive aggregation control shows higher molecular weight oligomeric bands.

Since none of the SDS concentrations used showed evidence for aggregation and we are interested in the most denaturing conditions, we further corroborated lack of aggregation at 30% SDS by testing if the CD spectra showed any sign of dependence on rhodopsin concentration. CD spectra of rhodopsin denatured with 30% SDS were recorded at increasing protein concentrations of 1.5μM, 5μM and 8μM. There was little if no dependence of MRE at 222nm on protein concentration (Figure 2.B.). This further supports the absence of aggregation at the maximum SDS concentration used (30%), even at higher rhodopsin concentrations.

Finally, we further corroborated the lack of aggregation in SDS using ^{1}H NMR spectroscopy.Proton peaks arising from a natively folded protein are dispersed across the range of approximately -1ppm to 10ppm. Peaks corresponding to amide protons are found mainly in the region from 6.5ppm to 10ppm. For a disordered or completely unfolded protein, all amide protons in similar chemical environment cluster together around 8ppm impairing resolution. In case of aggregated protein, loss of peak dispersion accompanied by an increase in line widths of proton peaks are expected. We therefore further checked for the lack of aggregation in SDS denatured states by recording one dimensional proton NMR spectra of rhodopsin in the absence and presence of SDS. To avoid interference from detergent signals, these spectra were obtained by selective excitation of the protein backbone region by using a sculpting scheme as described in (37,38). Overlay of the proton spectra,

showing the backbone region of rhodopsin alone and in the presence of 1% SDS is displayed in Figure 2.C. The peaks in native rhodopsin correspond mostly to the flexible regions of rhodopsin that become sharper on adding 1% SDS. The peaks between 7.2ppm and 6.8ppm in the native state coalesce to form a sharper peak in 1% SDS denatured state. Figure 2.D. shows the overlay between native rhodopsin and that in presence of 30% SDS. Here again the peaks become sharper in presence of 30% SDS compared to the native state. Peaks between 7.2ppm and 6.8ppm appear to merge giving rise to a sharper peak in presence of 30% SDS. However, the overall peak intensity suffers a decrease in presence of 30% SDS when compared to that of native rhodopsin. This may be due to slow tumbling of the large cylindrical SDS micelles that are formed at 30% SDS. These 1D spectra show absence of aggregation since an aggregated protein sample would have given rise to broad peaks. No significant changes were seen in these spectra even after four days indicating absence of any time dependent aggregation (Figures 2.E. and 2.F.).

Urea as a denaturant of rhodopsin: disruption of secondary structure

Next, we measured the effect of urea on rhodopsin by CD spectroscopy. Rhodopsin (1.5μM) was titrated with different concentrations of urea and the CD spectrum was recorded at each concentration, as shown in Figure 3.A. The change in MRE at 222nm as a function of urea concentration is shown in Figure 3.B. A two-stage unfolding behavior was observed. Essentially, no change in secondary structure of rhodopsin occurs up to 6M urea. This is followed by a steep decrease by 57% in the magnitude of MRE at 222nm in the range between 6M and 10M urea. This is greater than the extent of denaturation by 30% SDS. The mid-point of the unfolding transition is at 7M urea. No time-dependent change in ellipticity was observed when rhodopsin was incubated with 10M urea for 12h (data not shown).

Urea as a denaturant of rhodopsin: Detection of aggregates

Urea denaturation disrupts helical content of rhodopsin to a large extent (see above). These largely unfolded states will be suitable for further analyses only if aggregation does not occur. Thus, we checked for aggregation in presence of urea by two methods, SDS-PAGE and dependence of MRE at 222nm on rhodopsin concentration.

Rhodopsin treated with different concentrations of urea was run on SDS-PAGE to check for aggregation as shown in Figure 4. Native gel loading dye was used to run urea containing rhodopsin samples so that SDS present in Laemmli dye does not influence our results (see Experimental Procedures). The second lane in Figure 4.A. corresponds to native rhodopsin. In subsequent lanes, rhodopsin immediately after addition of 4M, 6M, 7M and 8M urea are shown. Oligomeric bands were seen from 7M urea denaturation onwards. This is also the urea concentration at which urea begins to significantly unfold rhodopsin (see Figure 3). Thus, we conclude that rhodopsin begins to aggregate as soon as urea starts to unfold it. Stability of urea denatured states was determined by incubating 1.5μM rhodopsin with 8M urea for 0h (lane 2), 24h (lane 3) and 48h (lane 4) (Figure 4.B.). The time course of urea denaturation clearly shows aggregation becoming worse with time. Increase in the extent of aggregation with increase in rhodopsin concentration denatured by 8M urea was seen by comparing lanes 1 (5μM rhodopsin) and 2 (8μM rhodopsin) in Figure 4.C. with that of rhodopsin at 1.5μM in lane 2 in Figure 4.B.

Dependence of MRE at 222nm on rhodopsin concentration in presence of 8M urea was analyzed also by CD spectroscopy. As shown above, aggregation is observed on the gel from 7M urea denaturation onwards. We therefore chose a concentration of 8M urea for this experiment. Thus, we denatured rhodopsin at increasing concentrations of 1.5μM, 5μM and 8μM with 8M urea. The CD spectrum at each of the rhodopsin concentrations was recorded (data not shown). However, precipitates already were detected by eye when 8μM rhodopsin

was treated with 8M urea indicating aggregation of rhodopsin and thus making further analysis by CD unnecessary. Thus, appearance of aggregates precludes the use of urea as a suitable denaturant for unfolding studies of rhodopsin.

3% SDS+8M urea mixture as a denaturant of rhodopsin: disruption of secondary structure

SDS caused a significant extent of denaturation of rhodopsin without causing aggregates whereas urea denatured secondary structure of rhodopsin to a greater extent than SDS but caused aggregation. We therefore tested if a mixed denaturant condition consisting of both, SDS and urea could result in an extent of denaturation similar or greater than that of urea but without aggregation. Concentrations of 3% SDS and 8M urea were chosen because addition of more than 3% SDS and 8M urea led to large increase in the total volume and dilution of the protein concentration. Also, 8M urea led to a similar degree of disruption of secondary structure as 10M urea, the latter being the maximum urea concentration that can be used. A 44% decrease in MRE at 222nm was observed when rhodopsin (1.5μM) was treated with 3% SDS followed by addition of 8M urea as indicated by the CD spectrum shown in Figure 5.A. A similar decrease in MRE at 222nm was also observed when rhodopsin was first treated with 8M urea followed by addition of 3% SDS (data not shown). Comparison of the extent of denaturation by 3% SDS (3S), 8M urea (8U), 3%SDS+8M urea (3S8U) and 30% SDS (30S) is shown in Figure 5.B. As can be seen in this figure, addition of 8M urea to 3% SDS denatured rhodopsin decreases the helicity to a much greater extent than that by 3% SDS alone. Also, the mixed denaturant leads to a similar extent of denaturation as that by 8M urea and is slightly greater than that by 30% SDS.

3% SDS+8M urea mixture as a denaturant of rhodopsin: Detection of aggregates

As described in the CD experiments above, the mixture of denaturants leads to a significant decrease in the secondary structure content of rhodopsin. To determine if this condition leads to aggregation, we ran the denatured samples on SDS-PAGE. In order to check for aggregation SDS-PAGE analysis was performed as shown in Figure 5.C. Samples were loaded using native dye (see Methods). Lane 2 shows presence of aggregates when rhodopsin is treated with 8M urea first followed by 3% SDS. This indicates irreversible aggregation by 8M urea that cannot be rescued by addition of 3% SDS. However, no aggregates were detected on addition of 3% SDS followed by 8M urea to rhodopsin, as shown in lane 3. Therefore, 3% SDS+8M urea, added in this order, is a suitable condition for studying denatured states of rhodopsin.

GuHCl and TFA as denaturants of rhodopsin: disruption of secondary structure

Two other denaturants, GuHCl and TFA were tested. The CD spectra of rhodopsin (1.5μM) titrated with different concentrations of GuHCl are shown in Figure 6.A. A plot of the change in MRE at 222nm as a function of GuHCl concentration is shown in Figure 6.B. Similar to the urea-induced denaturation, a two-stage behavior is seen on GuHCl unfolding. Here, the mid-point of transition was at 4M GuHCl, as compared to the mid-point of the unfolding transition in urea of 7M (see above). The decrease in MRE at 222nm at 8M GuHCl is 66%; no time-dependent decrease in helicity was observed when rhodopsin was incubated with 8M GuHCl for 12h (data not shown).

Finally, an organic solvent, TFA, known for its strong denaturing properties and previous denaturation power in the case of bacteriorhodopsin (18) was tested. 4M TFA was seen to disrupt rhodopsin almost completely as seen by the absence of a CD signal in the spectrum shown in Figure 6.A. However, 4M TFA buffer alone gave a strong CD signal, making the quantification of the signal unreliable. Lower concentrations of TFA were also tested. For example, TFA at a concentration of 100mM is the highest concentration with minimal signal

background. However, this concentration led to a relatively small decrease of only ~12% in MRE at 222nm (data not shown).

GuHCl and TFA as denaturants of rhodopsin: Detection of aggregates

GuHCl denaturation results in a large decrease in MRE at 222nm as seen from CD spectroscopy and TFA denaturation resulted in complete disappearance of the CD signal indicating complete disruption of secondary structure of rhodopsin. Thus, TFA could potentially be the best denaturant if it also does not cause aggregation. Unlike for other denaturing conditions described above, SDS-PAGE analysis could not be performed for GuHCl containing samples as precipitation was observed when Laemmlli buffer was added. Furthermore, native loading dye could not be used to run GuHCl denatured samples as they remained stuck in the wells of the gel. We therefore checked for aggregation under both GuHCl and TFA denaturation conditions by determining the dependence of MRE at 222nm on rhodopsin concentration. For GuHCl denaturation we also measured tryptophan fluorescence and accessibility of cysteine in denatured states.

The CD spectra of rhodopsin at different concentrations of 1.5μM, 3μM, 5μM, 6μM, 7μM and 8μM each denatured with 6M and that of 1.5μM, 3μM, 5μM, 6μM and 8μM each denatured with 8M GuHCl were recorded. Dependence of the molar ellipticity at 222nm on protein concentration was observed at both 6M and 8M GuHCl concentrations tested (Figure 7.A.). This indicates that rhodopsin oligomerizes under these conditions and the greater decrease in MRE at 222nm that is observed in Figure 6 may be merely an aggregation effect.

To check for aggregation in TFA-denatured samples, different concentrations of rhodopsin at 1.5μM, 5μM and 8μM were denatured with 4M TFA and a CD spectrum was recorded for each of them. A dependence of MRE at 222nm on rhodopsin concentration was seen but it could not be clearly determined due to high absorbance at 222nm by buffer alone (data not shown). However, aggregates were clearly detected by eye after 3 days of preparing the samples.

Indirect evidence for aggregation in GuHCl also came from fluorescence spectroscopy. There are five tryptophan residues in rhodopsin. Their fluorescence in dark-adapted rhodopsin is quenched due to energy transfer to the retinal chromophore. The release of retinal, e.g. following light-activation and decay of the activated Metarhodopsin II species to free retinal and opsin, causes an increase in tryptophan fluorescence (41). Thus, fluorescence spectroscopy of rhodopsin is a sensitive probe for rhodopsin structure. Furthermore, aggregation would be expected to decrease rhodopsin fluorescence by way of quenching of tryptophan fluorescence through inter-molecular interactions. The changes in tryptophan fluorescence intensity at 330nm as a function of GuHCl concentration are plotted in Figure 7.B. An initial increase in tryptophan fluorescence was seen up to 3M GuHCl. This is consistent with the disruption of retinal-protein interaction as the protein begins to unfold, similar to what would be seen by the retinal leaving the binding pocket after light-activation. With further increase in GuHCl concentration up to 8M, a decrease in fluorescence counts was observed. This is contrary to the significant unfolding of rhodopsin that occurs in the range 3M-8M GuHCl as judged by CD spectroscopy (see above). Therefore, this result supports the notion that rhodopsin aggregates under these conditions, which is expected to lead to a quenching of fluorescence. A similar pattern of change in fluorescence was also observed on longer incubation of rhodopsin with GuHCl (Figure 7.B.).

Finally, we also investigated aggregation indirectly through protein accessibility measurements. Analogous to fluorescence measurements, tertiary structure and aggregation of rhodopsin can be probed by cysteine accessibility. Accessibility of cysteine residues was probed using the cysteine derivatizing agent, 4,4’-dithiodipyridine (4-PDS). 4-PDS reacts

with the accessible free sulfhydryl groups of cysteines releasing stoichiometric amounts of 4-thiopyridone which has an absorption maximum at 323nm (39). Of the six free cysteines in rhodopsin, only two of them can be derivatized in the dark state whereas all six of them can be derivatized upon loss of 11-*cis* retinal on light activation (42). The effect on reactivity of cysteines to 4-PDS in GuHCl denatured states was checked. An increase in cysteine accessibility to four cysteines was seen up to 3M GuHCl (Figure 7.C.). Further increase in GuHCl concentration to 8M showed a decrease in the number of cysteines reacting with 4-PDS to three (Figure 7.C.). This pattern is similar to the decrease seen in tryptophan fluorescence. Burial of both tryptophans and cysteines, occurring at the same concentration of GuHCl, indicates formation of aggregates. Taken together, these experiments suggest that GuHCl and TFA are not suitable denaturants for characterizing unfolded states of rhodopsin due to their aggregation properties.

Discussion

Membrane proteins are notoriously difficult to unfold (19) due to the challenge of perturbing the surrounding stable membrane environment. In this paper we aimed at achieving a largely denatured state of rhodopsin *in vitro* in order to mimic what might be corresponding to an *in vivo* early unfolded intermediate. Computational and single molecule studies with the mammalian membrane protein rhodopsin have suggested that complex folding mechanisms may have to be considered to describe the folding of this protein (16,17,43,44). Thus, in-depth studies of denatured states are needed to better understand these mechanisms. The characterization of unfolded states of rhodopsin, however is still in a preliminary stage. The present paper aims to systematically compare different denaturing conditions with the aim of identifying conditions that maximally denature rhodopsin without aggregation. Because detergents such as DM do not interfere with spectroscopic techniques as compared to other membrane mimetics, we conducted all our studies with rhodopsin reconstituted in DM. DM is a favorable detergent for rhodopsin studies because it maintains maximum rhodopsin function (45,46). Despite the spectroscopic and functional advantages of using DM, the thermal stability of rhodopsin in DM micelles is the same as compared to that in native membranes (47,48). While this is favorable for ensuring functional relevance of measurements in DM, it also makes it equally difficult to study unfolding of rhodopsin by *in vitro* denaturation experiments as if we were working with membranes. Here, we report the results of screening different denaturants to arrive at conditions that lead to maximum unfolding of rhodopsin without causing its aggregation. The former was assessed by CD spectroscopy and the latter by different techniques depending on the suitability for the specific denaturant under investigation.

The use of CD spectroscopy for determining extent of denaturation was mostly qualitative because of the known interference of aggregation. Therefore, MRE at 222nm was mainly used to report on the degree of disruption of secondary structure instead of calculating percent helicity by deconvoluting the CD spectra. MRE at 222nm is strongly influenced by conformation of residues in a helix, length of helix, number of helices, distribution of residues in these helices, fluctuations of a helix and the dielectric constant of the surrounding medium (49,50). These parameters have an important contribution towards helicity estimation in the case of denatured proteins. However, in the absence of suitable basis sets for denatured membrane proteins, compared to which software such as CDPro estimate the helicity (33), it is difficult to derive these parameters quantitatively from CD spectra. We therefore primarily relied on MRE at 222nm values to describe secondary structure loss during denaturation in the Results section. Since it was found that basis sets in CDPro containing only soluble proteins when used for quantifying secondary structure of membrane proteins yield reasonably accurate, albeit not quantitative results when considering α-helix content alone, we did estimate the extent of decrease in helicity as a

qualitative indicator of the extent of unwinding of helices. This would provide the reader with some qualitative indication about the extent of denaturation being achieved.

SDS as a denaturant

SDS has been commonly used as a denaturant for both, membrane proteins (26,27,51,52) and soluble proteins (53-58). It was shown that the modes of unfolding depend on the SDS concentration range used and indeed SDS induced unfolding of soluble proteins correlates with changes in SDS micellar structure (59,60). At low concentrations of up to 100mM, SDS forms spherical micelles which convert into cylindrical micelles at concentrations above 6% where the aggregation number of SDS increases from 63 to 91 (61). These cylindrical micelles, also referred to as “mode 2” micelles, are known to have more aggressive protein denaturation properties than the cylindrical micelles (60). Rapid unfolding occurs in this mode due to the large number of SDS molecules interacting with the protein and enveloping it in its large cylindrical structures. Under high SDS concentration conditions, the transition state is stabilized and thus the energy barrier to unfolding is decreased.

Because native rhodopsin as a membrane protein is maintained in DM detergent micelles, we propose that we expect four stages in detergent properties based on these published SDS properties. These stages are visualized schematically in Figure 8. At low concentrations of SDS, we expect that the SDS displaces the DM molecules in the micelles to form SDS/DM mixed micelles. Thus, stage 1 (0.05% to 0.3% SDS) represents spherical DM/SDS mixed micelles. As the SDS concentration increases, the contribution of the relatively small concentration of DM decreases, so that stage 2 (0.3% to 3% SDS) is dominated by the vast excess of SDS in the spherical micelles. Stage 3 (3% to 10% SDS) marks the transition from spherical to cylindrical SDS micelle shapes. Stage 4 (15% to 30% SDS) is then dominated by the cylindrical micellar structures of SDS. [Note that the use of the word “stages” merely intends to reference the different ranges in SDS concentration, and does not imply a temporal progression of rhodopsin structure during denaturation.]

Below, we discuss our rhodopsin denaturation by SDS in light of these stages. In the first stage of unfolding, at low [SDS] of 0.05% to 0.3%, a modest decrease in the magnitude of MRE at 222nm was seen which saturated at a value of ~12% in stage 2 at [SDS] up to 3%, which corresponds to 100mM. Stage 3 is a transition, when SDS is going from spherical to cylindrical “mode 2” micelles (see Figure 8) (61). SDS concentrations between 3% (100mM) and 15% (500mM) form this stage as the increase in aggregation number of SDS beyond 6% (200mM) leads to very large number of SDS molecules interacting with rhodopsin. As a result, we see an increase in the magnitude of MRE at 222nm at 10% SDS to a value close to the native state indicating that SDS is inducing non-native helices, a well-known property of SDS. Stage 4 is then dominated by cylindrical micellar structures of SDS (see Figure 8) that surround largely unfolded states of rhodopsin. Here, we see a ~40% decrease in MRE at 222nm at 30% SDS (1M). We estimate the extent of decrease in helicity on adding 30% SDS as a qualitative indicator of the extent of unwinding of helices, and obtained a value of approximately 45%. This is consistent with “mode 2” unfolding in which SDS cylindrical micelles wrap around the membrane protein and aggressively unfold it (59,60). Formation of cylindrical micelles by SDS is also supported by 1D ^{1}H NMR experiments. A decrease in overall peak intensities of 30% SDS denatured rhodopsin as compared to the native form can be attributed to slow tumbling of the large cylindrical micelles that are formed at such high SDS concentrations.

In order for SDS denatured conditions to qualify for biophysical studies of denatured rhodopsin, we checked for aggregation. No aggregation of rhodopsin was detected based on multiple lines of evidences. SDS denatured rhodopsin did not show any oligomeric bands on

SDS-PAGE. By using CD spectroscopy, a dependence of ellipticity at 222nm on protein concentration would be expected if there are aggregates forming. Such dependence was not seen when rhodopsin at different concentrations was denatured by 30% SDS, the maximum concentration of SDS used here. Further, proton peaks on NMR spectrum of SDS denatured rhodopsin did not show any significant broadening compared to its native state, even after four days of incubation with 1% and 30% SDS the spectrum remained almost the same. However, there was a decrease in overall signal intensity of 30% SDS denatured state compared to the native state. This may be due to formation of cylindrical micelles of SDS which tumble slowly or technical difficulties due to the high buffer concentrations or protein aggregation. Since, aggregation has been ruled out by SDS-PAGE and CD spectroscopy, and no peak broadening was seen on NMR spectra of SDS treated rhodopsin, we conclude that the decreased intensity of the proton peaks is not due to aggregation. This is consistent with the notion that aggregation of rhodopsin, being a membrane protein, is less likely in the presence of SDS because even though SDS is denaturing, it does provide a hydrophobic environment. Here, the hydrophobic amino acids that will be exposed due to unfolding still remain surrounded by the hydrophobic tails of SDS and thus are shielded from the aqueous medium preventing aggregation. These results indicate that the maximum concentration of SDS of 30% is a desirable condition for future unfolding studies of rhodopsin.

Urea as a denaturant

Urea has been used very recently to study denaturation of opsin, a retinal-free form of rhodopsin, in phospholipid/detergent bicelles where it was shown to irreversibly unfold opsin to a significant extent (31). It was shown that 4M urea could denature opsin to a significant extent as measured by a decrease in MRE at 222nm by ~50%. In our study also, a significant degree of unfolding of rhodopsin in DM micelles with urea is seen but at a much higher concentration of urea i.e. 8M urea could decrease MRE at 222nm by 57%. This is mostly due to differences in the degree of intrinsic stability of opsin and rhodopsin which is also influenced by the micellar system in which they are reconstituted. It appears that the native state of opsin is less stable than that of rhodopsin. It is also possible that urea-denatured opsin is less prone to aggregation because no precipitates by eye and change in sample absorbance, reported by voltage changes in the photomultiplier tube, occurred during time course studies by CD indicating absence of light scattering and hence aggregation (31). We found this method to be less reliable in detecting aggregation in our studies because they only detect very large aggregates. While we also did not detect aggregation by these methods in our studies, we did detect them based on SDS-PAGE and analysis by eye at higher rhodopsin concentrations. It is likely that aggregation is caused by exposure of large hydrophobic regions of rhodopsin due to its unfolding in urea. A way to mask these hydrophobic parts of the protein could prevent it from oligomerizing. For this reason, we tested a mixture of 8M urea and 3% SDS as a denaturant so that SDS can be effective in screening the hydrophobic residues from water. While aggregates are detected when 3% SDS was added to 8M urea denatured rhodopsin, no aggregates are detected on reversing the order of addition of the denaturants. This further supports our theory that the cause of aggregation of rhodopsin in 8M urea is exposure of hydrophobic parts, which if masked by SDS before being denatured by 8M urea does not lead to aggregation. The extent of denaturation in 3% SDS+8M urea is found to be similar to that by 8M urea and slightly greater than that by 30% SDS thus making it a favorable denaturing condition to study unfolded states.

GuHCl and TFA as denaturants

GuHCl denaturation leads to a decrease in MRE at 222nm of rhodopsin by a greater extent compared to the above mentioned denaturing conditions. TFA, a strong denaturing condition, leads to the maximum decrease in MRE at 222nm compared to all of the

denaturants tested. It leads to a complete disappearance of CD signal indicating complete unfolding of secondary structure. However, both these conditions also lead to formation of aggregates thus impairing their use in further unfolding studies. For GuHCl denaturation, MRE at 222nm depended on rhodopsin concentration indicating aggregation. TFA induced unfolding led to precipitation after 3 days of TFA addition to rhodopsin indicating aggregation. The cause of aggregation is again likely due to the exposure of hydrophobic residues as with urea. However, SDS could not be added to mask exposed hydrophobic amino acids so that aggregation can be prevented, since precipitation occurred when SDS and GuHCl buffers were mixed together.

Conclusions

In this paper, we have screened different denaturing conditions, SDS, urea, SDS+urea, GuHCl and TFA for maximum unfolding without formation of aggregates. Rhodopsin denaturation is measured in terms of decrease in MRE at 222nm. TFA denatured rhodopsin to the maximum extent (~100%) compared to all the denaturants tested but led to aggregation precluding its use as a good denaturant. GuHCl was the next best at denaturing rhodopsin (66% decrease in MRE at 222nm) followed by urea (57% decrease in MRE at 222nm) but rhodopsin aggregated under both these conditions. Thus, urea and GuHCl, which are effective denaturants for soluble proteins, are not ideally suited for studying folding mechanisms of the membrane protein rhodopsin. 30% SDS proved to be a suitable denaturing condition as it denatured rhodopsin significantly (40% decrease in MRE at 222nm) without aggregating it. Also, the mixture of 3% SDS and 8M urea is a favourable condition as it denatures rhodopsin to a similar extent as that by 30% SDS (44% decrease in MRE at 222nm) and does not aggregate it. We conclude that SDS, either alone or in combination with urea, is a very suitable denaturant, due to the large degree of unfolding of rhodopsin in its presence and due to its ability to mask exposed hydrophobic stretches of largely unfolded membrane protein by its long hydrocarbon tails, thus preventing them from aggregation.

It is an important open question for soluble and membrane proteins alike to what extent unfolded states exist at all and in particular in vivo. Theoretical considerations suggest that a fully unfolded denatured state does not exist (62) and proteins are known to fold co-translationally (63,64). For membrane proteins, folding within the translocon has to be considered in addition. However, folding in solution and in the translocon seem to share similarities (65), and understanding the unfolded states is important in understanding what drives membrane protein folding. Thus, there is much to be learnt from the investigation of unfolded states of membrane proteins *in vitro*. Since it is unlikely that a completely unfolded state exists *in vivo* within a membrane environment, deciphering where the regions with highest propensity for residual structure in membrane proteins are located, is expected to shed light on understanding the mechanisms of membrane protein folding *in vitro* and *in vivo*.

Abbreviations

SDS	sodium dodecyl sulfate
DM	dodecyl maltoside
PDS	4,4′-Dipyridyldisulfide (alternative name: 4,4’-Dithiodipyridine)
CD	circular dichroism
MRE	mean residue ellipticity

TFA	trifluoroacetic acid
GuHCl	guanidine hydrochloride

References

1. Takeda S, Kadowaki S, Haga T, Takaesu H, Mitaku S. Identification of G protein-coupled receptor genes from the human genome sequence. FEBS Lett. 2002; 520:97–101. [PubMed: 12044878]
2. Sanders CR, Myers JK. Disease-related misassembly of membrane proteins. Annu. Rev. Biophys. Biomol. Struct. 2004; 33:25–51. [PubMed: 15139803]
3. Chiti F, Dobson CM. Amyloid formation by globular proteins under native conditions. Nat. Chem. Biol. 2009; 5:15–22. [PubMed: 19088715]
4. Dobson CM. The structural basis of protein folding and its links with human disease. Philos. Trans. R. Soc. Lond. B Biol. Sci. 2001; 356:133–145. [PubMed: 11260793]
5. Klein-Seetharaman J, Oikawa M, Grimshaw SB, Wirmer J, Duchardt E, Ueda T, Imoto T, Smith LJ, Dobson CM, Schwalbe H. Long-range interactions within a nonnative protein. Science. 2002; 295:1719–1722. [PubMed: 11872841]
6. Harper JD, Lansbury PT Jr. Models of amyloid seeding in Alzheimer's disease and scrapie: mechanistic truths and physiological consequences of the time-dependent solubility of amyloid proteins. Annu. Rev. Biochem. 1997; 66:385–407. [PubMed: 9242912]
7. Booth DR, Sunde M, Bellotti V, Robinson CV, Hutchinson WL, Fraser PE, Hawkins PN, Dobson CM, Radford SE, Blake CC, Pepys MB. Instability, unfolding and aggregation of human lysozyme variants underlying amyloid fibrillogenesis. Nature. 1997; 385:787–793. [PubMed: 9039909]
8. Sekijima Y, Wiseman RL, Matteson J, Hammarstrom P, Miller SR, Sawkar AR, Balch WE, Kelly JW. The biological and chemical basis for tissue-selective amyloid disease. Cell. 2005; 121:73–85. [PubMed: 15820680]
9. Canet D, Sunde M, Last AM, Miranker A, Spencer A, Robinson CV, Dobson CM. Mechanistic studies of the folding of human lysozyme and the origin of amyloidogenic behavior in its disease-related variants. Biochemistry. 1999; 38:6419–6427. [PubMed: 10350460]
10. Soto C, Sigurdsson EM, Morelli L, Kumar RA, Castano EM, Frangione B. Beta-sheet breaker peptides inhibit fibrillogenesis in a rat brain model of amyloidosis: implications for Alzheimer's therapy. Nat. Med. 1998; 4:822–826. [PubMed: 9662374]
11. Johnson SM, Wiseman RL, Sekijima Y, Green NS, Adamski-Werner SL, Kelly JW. Native state kinetic stabilization as a strategy to ameliorate protein misfolding diseases: a focus on the transthyretin amyloidoses. Acc. Chem. Res. 2005; 38:911–921. [PubMed: 16359163]
12. Ray SS, Nowak RJ, Brown RH Jr. Lansbury PT Jr. Small-molecule-mediated stabilization of familial amyotrophic lateral sclerosis-linked superoxide dismutase mutants against unfolding and aggregation. Proc. Natl. Acad. Sci. U. S. A. 2005; 102:3639–3644. [PubMed: 15738401]
13. Soldi G, Plakoutsi G, Taddei N, Chiti F. Stabilization of a native protein mediated by ligand binding inhibits amyloid formation independently of the aggregation pathway. J. Med. Chem. 2006; 49:6057–6064. [PubMed: 17004719]
14. Popot JL, Engelman DM. Membrane protein folding and oligomerization: the two-stage model. Biochemistry. 1990; 29:4031–4037. [PubMed: 1694455]
15. Engelman DM, Chen Y, Chin CN, Curran AR, Dixon AM, Dupuy AD, Lee AS, Lehnert U, Matthews EE, Reshetnyak YK, Senes A, Popot JL. Membrane protein folding: beyond the two stage model. FEBS Lett. 2003; 555:122–125. [PubMed: 14630331]
16. Klein-Seetharaman J. Dual role of interactions between membranous and soluble portions of helical membrane receptors for folding and signaling. Trends. Pharmacol. Sci. 2005; 26:183–189. [PubMed: 15808342]
17. Tastan O, Yu E, Ganapathiraju M, Aref A, Rader AJ, Klein-Seetharaman J. Comparison of stability predictions and simulated unfolding of rhodopsin structures. Photochem. Photobiol. 2007; 83:351–363. [PubMed: 17576347]

18. Huang KS, Bayley H, Liao MJ, London E, Khorana HG. Refolding of an integral membrane protein. Denaturation, renaturation, and reconstitution of intact bacteriorhodopsin and two proteolytic fragments. J. Biol. Chem. 1981; 256:3802–3809. [PubMed: 7217055]
19. Booth PJ, Curnow P. Membrane proteins shape up: understanding in vitro folding. Curr. Opin. Struct. Biol. 2006; 16:480–488. [PubMed: 16815700]
20. Booth PJ, Flitsch SL, Stern LJ, Greenhalgh DA, Kim PS, Khorana HG. Intermediates in the folding of the membrane protein bacteriorhodopsin. Nat. Struct. Biol. 1995; 2:139–143. [PubMed: 7749918]
21. Riley ML, Wallace BA, Flitsch SL, Booth PJ. Slow alpha helix formation during folding of a membrane protein. Biochemistry. 1997; 36:192–196. [PubMed: 8993333]
22. Booth PJ, Farooq A. Intermediates in the assembly of bacteriorhodopsin investigated by time-resolved absorption spectroscopy. Eur. J. Biochem. 1997; 246:674–680. [PubMed: 9219525]
23. Booth PJ, Farooq A, Flitsch SL. Retinal binding during folding and assembly of the membrane protein bacteriorhodopsin. Biochemistry. 1996; 35:5902–5909. [PubMed: 8639552]
24. Allen SJ, Curran AR, Templer RH, Meijberg W, Booth PJ. Folding kinetics of an alpha helical membrane protein in phospholipid bilayer vesicles. J. Mol. Biol. 2004; 342:1279–1291. [PubMed: 15351651]
25. Barrera FN, Renart ML, Molina ML, Poveda JA, Encinar JA, Fernandez AM, Neira JL, Gonzalez-Ros JM. Unfolding and refolding in vitro of a tetrameric, alpha-helical membrane protein: the prokaryotic potassium channel KcsA. Biochemistry. 2005; 44:14344–14352. [PubMed: 16245951]
26. Lau FW, Bowie JU. A method for assessing the stability of a membrane protein. Biochemistry. 1997; 36:5884–5892. [PubMed: 9153430]
27. Otzen DE. Folding of DsbB in mixed micelles: a kinetic analysis of the stability of a bacterial membrane protein. J. Mol. Biol. 2003; 330:641–649. [PubMed: 12850136]
28. Miller D, Charalambous K, Rotem D, Schuldiner S, Curnow P, Booth PJ. In vitro unfolding and refolding of the small multidrug transporter EmrE. J. Mol. Biol. 2009; 393:815–832. [PubMed: 19699749]
29. Dockter C, Volkov A, Bauer C, Polyhach Y, Joly-Lopez Z, Jeschke G, Paulsen H. Refolding of the integral membrane protein light-harvesting complex II monitored by pulse EPR. Proc. Natl. Acad. Sci. U. S. A. 2009; 106:18485–18490. [PubMed: 19833872]
30. Plumley FG, Schmidt GW. Reconstitution of chlorophyll a/b light-harvesting complexes: Xanthophyll-dependent assembly and energy transfer. Proc. Natl. Acad. Sci. U. S. A. 1987; 84:146–150. [PubMed: 16593794]
31. McKibbin C, Farmer NA, Edwards PC, Villa C, Booth PJ. Urea unfolding of opsin in phospholipid bicelles. Photochem. Photobiol. 2009; 85:494–500. [PubMed: 19192206]
32. Oprian DD, Molday RS, Kaufman RJ, Khorana HG. Expression of a synthetic bovine rhodopsin gene in monkey kidney cells. Proc. Natl. Acad. Sci. U. S. A. 1987; 84:8874–8878. [PubMed: 2962193]
33. Sreerama, N. a. W.; R.W.. Estimation of Protein Secondary Structure from Circular Dichroism Spectra: Comparison of CONTIN, SELCON, and CDSSTR Methods with an Expanded Reference Set. Anal. Biochem. 2000; 287:252–260. [PubMed: 11112271]
34. Provencher SW, Glockner J. Estimation of globular protein secondary structure from circular dichroism. Biochemistry. 1981; 20:33–37. [PubMed: 7470476]
35. Sreerama N, Woody RW. A self-consistent method for the analysis of protein secondary structure from circular dichroism. Anal. Biochem. 1993; 209:32–44. [PubMed: 8465960]
36. Manavalan P, Johnson WC Jr. Variable selection method improves the prediction of protein secondary structure from circular dichroism spectra. Anal. Biochem. 1987; 167:76–85. [PubMed: 3434802]
37. Hwang TL, Shaka AJ. Water Suppression That Works. Excitation Sculpting Using Arbitrary Wave-Forms and Pulsed-Field Gradients. J. Magn. Reson. A. 1995; 112:275–279.
38. Stott K, Stonehouse J, Keeler J, Hwang T-L, Shaka AJ. Excitation Sculpting in High-Resolution Nuclear Magnetic Resonance Spectroscopy: Application to Selective NOE Experiments. J. Am. Chem. Soc. 1995; 117:4199–4200.

39. Grassetti DR, Murray JF Jr. Determination of sulfhydryl groups with 2,2'- or 4,4'-dithiodipyridine. Arch. Biochem. Biophys. 1967; 119:41–49. [PubMed: 6052434]
40. Klein-Seetharaman J, Hwa J, Cai K, Altenbach C, Hubbell WL, Khorana HG. Single-cysteine substitution mutants at amino acid positions 55-75, the sequence connecting the cytoplasmic ends of helices I and II in rhodopsin: reactivity of the sulfhydryl groups and their derivatives identifies a tertiary structure that changes upon light-activation. Biochemistry. 1999; 38:7938–7944. [PubMed: 10387036]
41. Farrens DL, Khorana HG. Structure and function in rhodopsin. Measurement of the rate of metarhodopsin II decay by fluorescence spectroscopy. J. Biol. Chem. 1995; 270:5073–5076. [PubMed: 7890614]
42. Chen YS, Hubbell WL. Reactions of the sulfhydryl groups of membrane-bound bovine rhodopsin. Membr. Biochem. 1978; 1:107–130. [PubMed: 41159]
43. Muller DJ, Kessler M, Oesterhelt F, Moller C, Oesterhelt D, Gaub H. Stability of bacteriorhodopsin alpha-helices and loops analyzed by single-molecule force spectroscopy. Biophys. J. 2002; 83:3578–3588. [PubMed: 12496125]
44. Rader AJ, Anderson G, Isin B, Khorana HG, Bahar I, Klein-Seetharaman J. Identification of core amino acids stabilizing rhodopsin. Proc. Natl. Acad. Sci. U. S. A. 2004; 101:7246–7251. [PubMed: 15123809]
45. Klein-Seetharaman J, Getmanova EV, Loewen MC, Reeves PJ, Khorana HG. NMR spectroscopy in studies of light-induced structural changes in mammalian rhodopsin: applicability of solution (19)F NMR. Proc. Natl. Acad. Sci. U. S. A. 1999; 96:13744–13749. [PubMed: 10570143]
46. Kusnetzow AK, Altenbach C, Hubbell WL. Conformational states and dynamics of rhodopsin in micelles and bilayers. Biochemistry. 2006; 45:5538–5550. [PubMed: 16634635]
47. Knudsen P, Hubbell WL. Stability of rhodopsin in detergent solutions. Membr. Biochem. 1978; 1:297–322. [PubMed: 228156]
48. Ramon E, Marron J, del Valle L, Bosch L, Andres A, Manyosa J, Garriga P. Effect of dodecyl maltoside detergent on rhodopsin stability and function. Vision Res. 2003; 43:3055–3061. [PubMed: 14611941]
49. Wallace BA, Lees JG, Orry AJ, Lobley A, Janes RW. Analyses of circular dichroism spectra of membrane proteins. Protein Sci. 2003; 12:875–884. [PubMed: 12649445]
50. Hirst JD, Brooks CL 3rd. Helicity, circular dichroism and molecular dynamics of proteins. J. Mol. Biol. 1994; 243:173–178. [PubMed: 7932747]
51. Dornmair K, Kiefer H, Jahnig F. Refolding of an integral membrane protein. OmpA of Escherichia coli. J. Biol. Chem. 1990; 265:18907–18911. [PubMed: 2229053]
52. London E, Khorana HG. Denaturation and renaturation of bacteriorhodopsin in detergents and lipid-detergent mixtures. J. Biol. Chem. 1982; 257:7003–7011. [PubMed: 7085614]
53. Ibel K, May RP, Kirschner K, Szadkowski H, Mascher E, Lundahl P. Protein-decorated micelle structure of sodium-dodecyl-sulfate--protein complexes as determined by neutron scattering. Eur. J. Biochem. 1990; 190:311–318. [PubMed: 2194800]
54. Jirgensons B. Effects of n-propyl alcohol and detergents on the optical rotatory dispersion of alpha-chymotrypsinogen, beta-casein, histone fraction F1, and soybean trypsin inhibitor. J. Biol. Chem. 1967; 242:912–918. [PubMed: 6067028]
55. Mascher E, Lundahl P. Sodium dodecyl sulphate-protein complexes : Changes in size or shape below the critical micelle concentration, as monitored by high-performance agarose gel chromatography. J. Chromatogr. A. 1989; 476:147–158.
56. Mattice WL, Riser JM, Clark DS. Conformational properties of the complexes formed by proteins and sodium dodecyl sulfate. Biochemistry. 1976; 15:4264–4272. [PubMed: 963036]
57. Rao JK, Argos P. Structural stability of halophilic proteins. Biochemistry. 1981; 20:6536–6543. [PubMed: 6796115]
58. Tanford, C. The Hydrophobic Effect. Formation of Micelles and Biological Membranes. 2nd. ed.. Wiley & Sons; New York: 1991.
59. Otzen DE. Protein unfolding in detergents: effect of micelle structure, ionic strength, pH, and temperature. Biophys. J. 2002; 83:2219–2230. [PubMed: 12324439]

60. Otzen DE, Oliveberg M. Burst-phase expansion of native protein prior to global unfolding in SDS. J. Mol. Biol. 2002; 315:1231–1240. [PubMed: 11827490]

61. Croonen Y, Gelade E, Van der Zegel M, Van der Auweraer M, Vandendriessche H, De Schryver FC, Almgren M. Influence of salt, detergent concentration, and temperature on the fluorescence quenching of 1-methylpyrene in sodium dodecyl sulfate with m-dicyanobenzene. J. Phys. Chem. 1983; 87:1426–1431.

62. Baldwin RL, Zimm BH. Are denatured proteins ever random coils? Proc. Natl. Acad. Sci. U. S. A. 2000; 97:12391–12392. [PubMed: 11070072]

63. Fedorov AN, Baldwin TO. Contribution of cotranslational folding to the rate of formation of native protein structure. Proc. Natl. Acad. Sci. U. S. A. 1995; 92:1227–1231. [PubMed: 7862665]

64. Makeyev EV, Kolb VA, Spirin AS. Enzymatic activity of the ribosome-bound nascent polypeptide. FEBS Lett. 1996; 378:166–170. [PubMed: 8549826]

65. Hessa T, Kim H, Bihlmaier K, Lundin C, Boekel J, Andersson H, Nilsson I, White SH, von Heijne G. Recognition of transmembrane helices by the endoplasmic reticulum translocon. Nature. 2005; 433:377–381. [PubMed: 15674282]

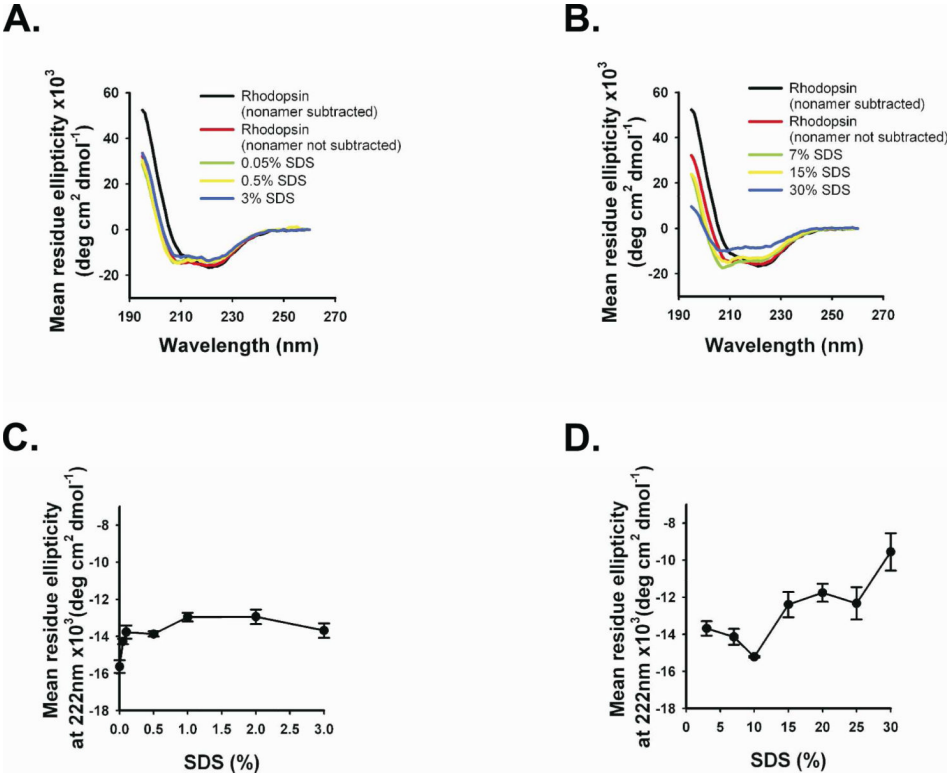

Figure 1.

SDS induced denaturation of rhodopsin monitored by CD spectroscopy. CD spectra of 1.5μM rhodopsin (black line) alone and in presence of A. 0.05%-3% and B. 7%-30% SDS concentrations. Total mean residue ellipticity at 222nm of rhodopsin in presence of C. 0.05%-3% SDS and that in presence of D. 7%-30% SDS. All CD spectra in 1.A. are subtracted from the corresponding buffer spectrum containing 70μM nonapeptide and those in Figure 1.B. are subtracted from buffer alone because of reasons stated in the Experimental Procedures section. Spectra of rhodopsin (nonamer not subtracted) correspond to a concentration of 1.5μM obtained after dilution from a very high concentrated protein sample thus resulting in amounts of nonamer undetectable by CD.

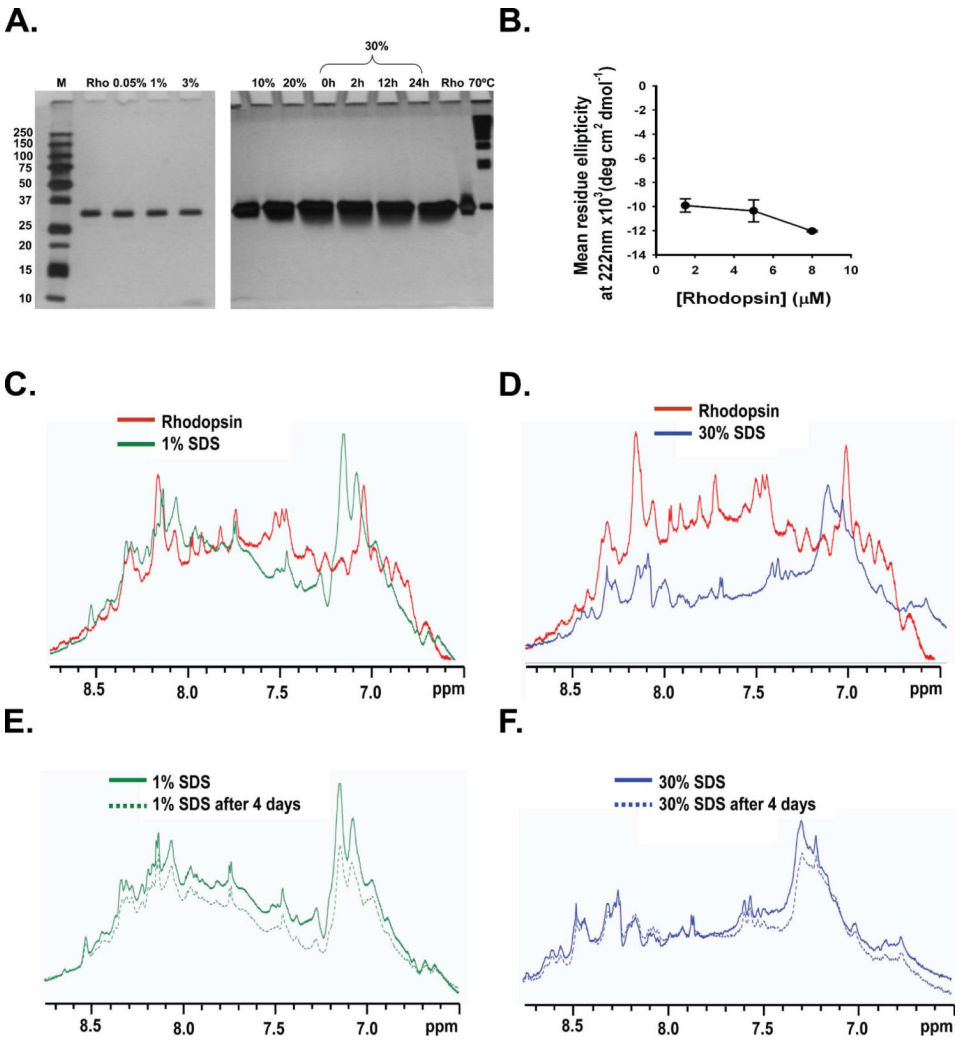

Figure 2.

A. Silver stained 10% SDS-polyacrylamide gel of rhodopsin in presence of SDS – first gel, Lane 1: marker, Lane 2: native rhodopsin, Lanes 3, 4, 5: rhodopsin in 0.05% SDS, 1% SDS and 3% SDS respectively and second gel, Lanes 2 and 3: rhodopsin in 10% and 20% SDS respectively, Lanes 4, 5, 6 and 7: rhodopsin in 30% SDS at time t=0h, 2h, 12h, 24h respectively, Lane 8: rhodopsin, Lane 9: rhodopsin denatured at 70°C. B. Plot showing changes in MRE at 222nm on rhodopsin concentration during SDS denaturation. 1D proton spectra showing overlay of C. rhodopsin and rhodopsin in 1% SDS, D. overlay of rhodopsin and rhodopsin in 30% SDS, E. overlay of rhodopsin in 1% SDS and F. 30% SDS after 4 days of incubation with that after immediate SDS addition.

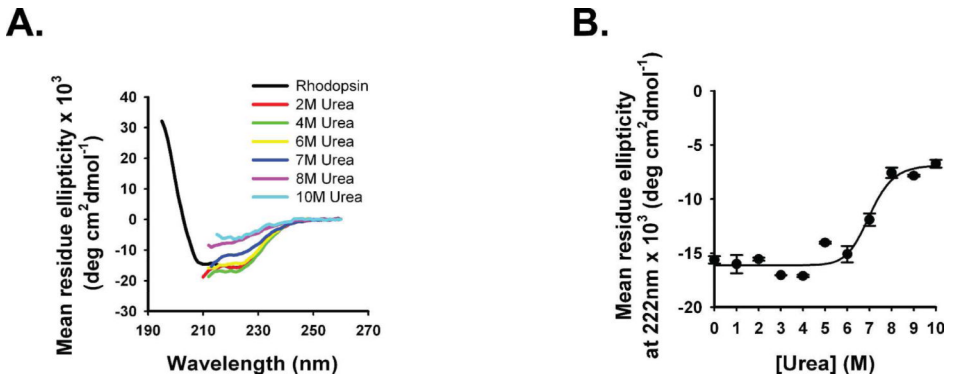

Figure 3.

Urea induced denaturation of rhodopsin monitored by CD spectroscopy. A. CD spectra of 1.5μM rhodopsin (black line) alone and in presence of urea concentration from 2M to 10M. B. Mean residue ellipticity at 222nm of rhodopsin in presence of 1M-10M urea.

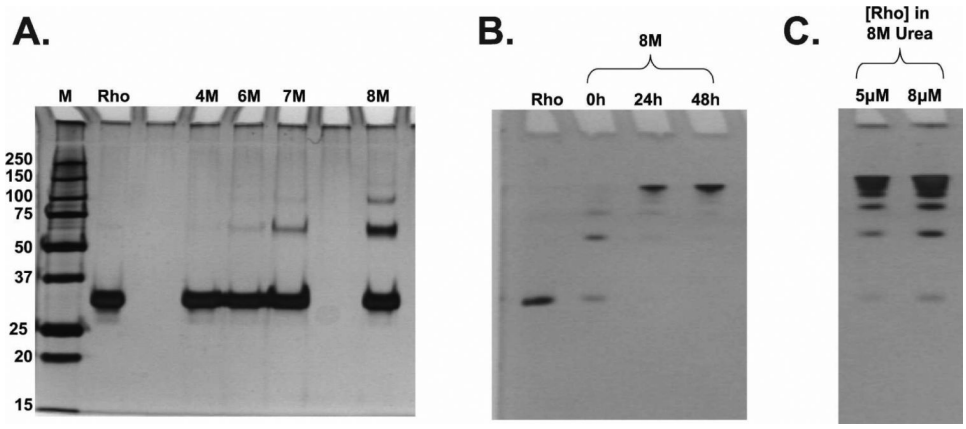

Figure 4.

Silver stained 10% SDS-polyacrylamide gel of rhodopsin in presence of different concentrations of urea. A. lane 1: marker, lane 2: native rhodopsin, lanes 3, 4, 5, 6: rhodopsin with 4M, 6M, 7M and 8M urea respectively after time t=0 of addition of urea.B. lane 2: native rhodopsin, lanes 3, 4, 5: 1.5μM rhodopsin in 8M urea after 0, 24h and 48h respectively. C. lanes 1 and 2: 5μM and 8μM rhodopsin with 8M urea respectively.

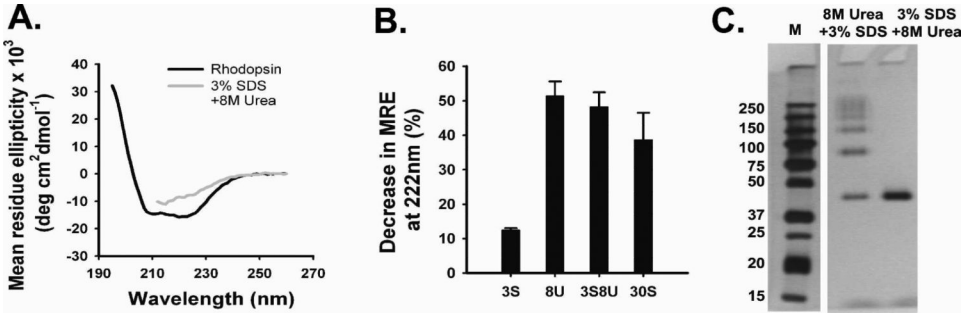

Figure 5.

3% SDS+8M urea induced denaturation of rhodopsin monitored by CD spectroscopy. A. CD spectra of 1.5μM rhodopsin (black line) alone and in presence of SDS+urea (grey line). B. Bar graph comparing percent decrease in MRE at 222nm under different denaturing conditions of 3% SDS (3S), 8M urea (8U), 3% SDS+8M urea (3S8U) and 30% SDS (30S). C. Silver stained 10% SDS-polyacrylamide gel of rhodopsin treated with 8M urea+3% SDS (8U3S) (lane 2) showing aggregation and 3% SDS+8M urea (3S8U) (lane 3) without any aggregates. Lane 1 shows the marker.

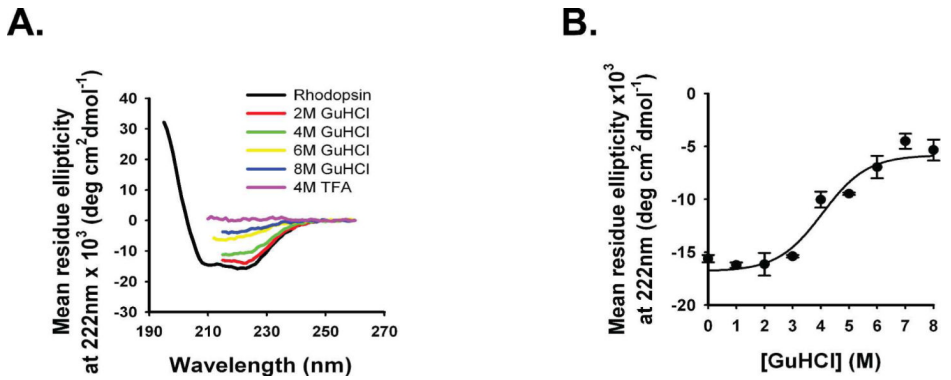

Figure 6.

GuHCl and TFA induced denaturation of rhodopsin monitored by CD spectroscopy. A. CD spectra of 1.5μM rhodopsin (black line) alone and in presence of GuHCl concentration from 2M to 8M and 4M TFA. B. Mean residue ellipticity at 222nm of rhodopsin in presence of 1-8M GuHCl.

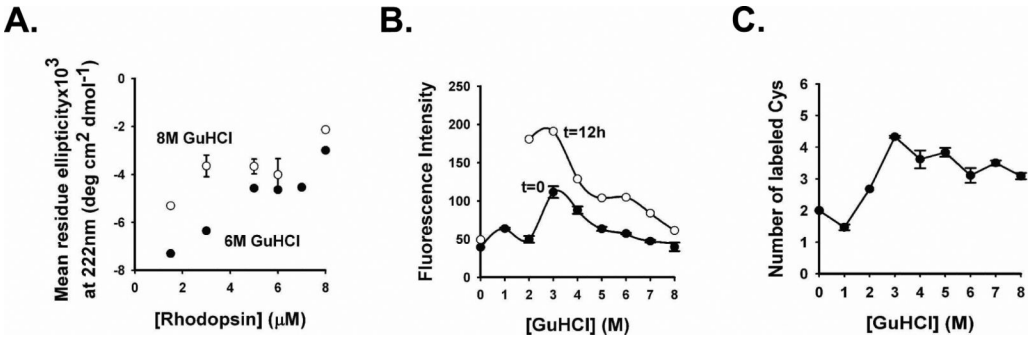

Figure 7.

Aggregation under GuHCl deanaturing condition. A. Plot showing linear dependence of MRE at 222nm on rhodopsin concentration on adding 6M (open circle) and 8M (filled circle) GuHCl. B. Changes in fluorescence intensity at 330nm in presence of 0-8M GuHCl immediately after its addition (filled circle) and after incubation for 12hrs (open circle). C. Number of cysteines reactive to 4-PDS in different concentration of GuHCl ranging from 0-8M.

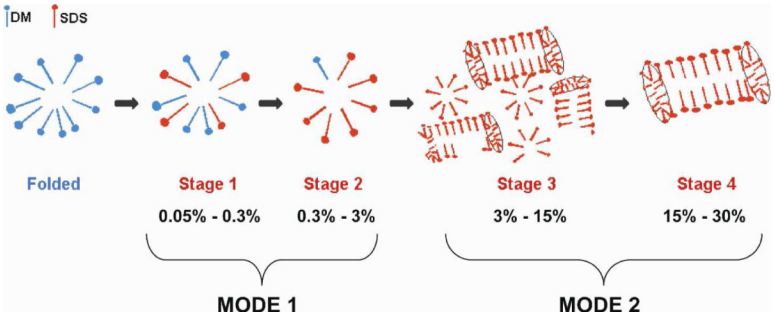

Figure 8.

Models representing changes in SDS (in red) micellar structure on increasing addition of SDS to DM (in blue) micelles. DM spherical micelles form DM/SDS mixed micelles in stage 1 upon SDS addition, stage 2 represents increase in SDS spherical micelles on further adding SDS, stage 3 represents transition to cylindrical micellar formation with further increase in [SDS], stage 4 represents formation of SDS cylindrical micelles.

Table 1

Summary of biophysical techniques used to detect aggregates

Denaturants	Concentration range	Techniques used for detection of aggregates					
		CD	**SDS-PAGE**	**NMR**	**Trp fluorescence**	**Cys accessibility**	**By eye**
SDS	0% - 30%	No dependence of MRE on [rhodopsin]	No oligomeric bands	No broad peaks representing aggregates	Shown in accompanying paper for analyses of tertiary structure changes	Shown in accompanying paper for analyses of tertiary structure changes	No precipitates detected
Urea	0M -10M	Not done since clear from SDS-PAGE and visual detection	Oligomeric bands	Cannot be done since aggregates are formed as seen by eye	Not done since sufficient evidence from SDS-PAGE and visual detection	Not done since sufficient evidence from SDS-PAGE and visual detection	Precipitates detected
SDS+Urea	3% SDS +8M urea	Not done since clear evidence from SDS-PAGE	No oligomeric bands, aggregation seen only when urea is added before adding SDS	Not done since clear evidence from SDS-PAGE	Not done since clear evidence from SDS-PAGE	Not done since clear evidence from SDS-PAGE	No precipitates detected
GuHC1	0M - 8M	Dependence of MRE on [rhodopsin]	GuHCl buffer alone precipitates on addition of Laemmlli dye	Cannot be done since aggregates are formed as seen by eye	Shows a decrease at 8M after an increase at 3M	Shows a decrease at 8M after an increase in 3M	Precipitates detected
TFA	100mM and 4M	Not done since precipitates were detected by eye and large background signals from buffer alone	Not done since precipitates were detected by eye	Cannot be done since aggregates are formed as seen by eye	Not done since precipitates were detected by eye	Not done since precipitates were detected by eye	Precipitates detected